

Measurements of intersubband photocurrents from quantum wells in asymmetrical-double-barrier structures

H. C. Liu, M. Buchanan, and Z. R. Wasilewski

*Institute for Microstructural Sciences, National Research Council,
Ottawa, Ontario, Canada K1A 0R6*

(Received 1 October 1990; Revised manuscript received 9 January 1991)

Photocurrents from quantum wells in asymmetrical-double-barrier resonant-tunneling structures are studied under $9\text{-}\mu\text{m}$ radiation. By use of intersubband transitions, large electron accumulations in the quantum wells are observed directly in one bias polarity, consistent with theory. This photon-assisted resonant-tunneling process may be used for fast-response infrared detection.

Studies of quantum-well (QW) structures for electronic and photonic applications are well known. The main research activities in QW photonic devices have been to utilize the *interband* (between conduction and valence bands) transition for lasers, detectors, and modulators in the near infrared (ir) to visible regions. Recently *intra*band (within a conduction or a valence band) or intersubband transitions in QW structures have been exploited for mid and far ir applications.¹⁻⁴ Another closely related current topic is the charge (electron) accumulation in a QW which gives rise to interesting observable effects.⁵⁻⁷ In this paper, we report on our experimental study of two asymmetrical-double-barrier resonant tunneling (RT) structures under $9\text{-}\mu\text{m}$ ir radiation from a CO_2 laser. Cai *et al.* used a Green's-function approach to calculate the photon-assisted RT through a double-barrier structure.⁸ The example in their calculation had relatively thin barriers, whereas the structures we study here have relatively thick barriers to reduce the dark current.

The basic idea is shown schematically in Fig. 1. We use asymmetrical-double-barrier RT structures with one barrier thicker than the other. When biased so that the thicker barrier is on the collector side (upper part in Fig. 1), we expect a large electron accumulation in the well.⁹ In the other bias polarity, we expect a negligible electron accumulation (lower part in Fig. 1). This can be easily understood in the following way. Let us view the tunneling as a two step process: (1) electrons from the emitter Fermi sea tunnel into the resonant state, and (2) electrons accumulated in the well (forming a two-dimensional electron gas) tunnel out to the collector. Under steady-state condition, the currents associated with the above two tunneling processes balance. If the collector barrier is less transparent than the emitter barrier, there must be a large electron density in the well in order to balance the current. Similarly, for the other bias polarity, a low density of electrons is expected in the well. We will make the argument more quantitative later. To observe the electron accumulation directly, we design the well so that the second resonant state is very close to the top of the barrier, and we use ir light to induce intersub-

band transitions and collect the photon-excited electrons as photocurrent. Because the tunneling out of the second resonant state has a high probability under bias and the electric field in the well is relatively small, the intersubband photocurrent is roughly proportional to the electron density in the well.

The two double-barrier structures, called samples No. 1 and 2, were grown by molecular-beam epitaxy on semi-insulating GaAs substrates. The double-barrier structure consists (in growth sequence) of a 700-nm bottom GaAs contact layer doped with Si to about $2.0 \times 10^{18} \text{ cm}^{-3}$, a 5.0-nm undoped GaAs spacer layer, a 10.0-nm $\text{Al}_{0.33}\text{Ga}_{0.67}\text{As}$ barrier, a 6.6-nm GaAs QW, a 14.0-nm $\text{Al}_{0.33}\text{Ga}_{0.67}\text{As}$ barrier, a 5.0-nm undoped GaAs spacer layer, and a 400-nm top GaAs contact layer doped with

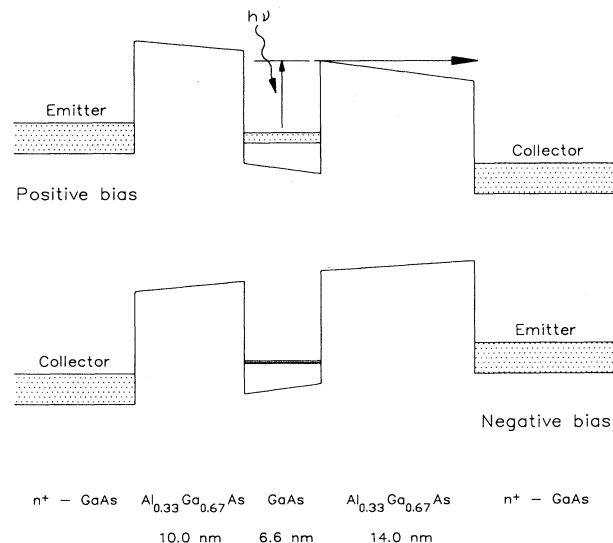


FIG. 1. Schematic forward and reverse bias potential profiles of the asymmetrical-double-barrier resonant-tunneling structure. A substantial electron accumulation occurs in the forward bias and an intersubband photocurrent is expected, while in the reverse bias the photocurrent should not be observable.

Si to about $2.0 \times 10^{18} \text{ cm}^{-3}$. The spacer layers are added to reduce diffusion and segregation of dopants from the heavily doped contact layers into the double barrier. The double-barrier region was not intentionally doped for sample No. 1, while the center of the well of sample No. 2 was δ doped with Si to about $9 \times 10^{11} \text{ cm}^{-2}$. X-ray rocking curves measuring an auxiliary superlattice grown before the double-barrier confirm that the growth conditions yielded the designed structural parameters. The well thickness (6.6 nm) and the barrier alloy fraction ($x = 0.33$) were chosen to give the energy difference between the ground and the first excited states coincident with $9\text{-}\mu\text{m}$ radiation photon energy. A 50 repeat multiple QW (MQW) sample with identical wells (6.6 nm) and barrier heights ($\text{Al}_{0.33}\text{Ga}_{0.67}\text{As}$) was also grown and tested, and showed a strong intersubband transition feature peaked at about $9 \mu\text{m}$. The barrier width of the MQW sample was 19.4 nm and the center of the wells was δ doped with Si to $9 \times 10^{11} \text{ cm}^{-2}$.

The $120 \times 120\text{-}\mu\text{m}^2$ square devices were defined by wet-chemical mesa etching, and had alloyed Ni/Ge/Au contacts. Facets of 45° were polished near the device mesas. Devices were mounted in a variable temperature optical cryostat equipped with an antireflection coated ZnSe window. A low power CO_2 laser together with a polarizer was used to observe the photocurrent. The measurement geometry and the definitions of the two polarizations (P

and S) are shown in the inset to Fig. 2. The polarized CW power density was varied in the range $0.01\text{--}0.5 \text{ W/cm}^2$. The ir light was incident normal to the facets. The photocurrent was measured across a $100\text{-}\Omega$ load resistor using a 1.5-KHz mechanical chopper and a lock-in amplifier. Device heating due to the current and the CO_2 radiation was negligible in the voltage and the power range of our experiment. The current versus voltage ($I\text{-}V$) and photocurrent versus bias voltage characteristics at about 10 K are shown in Fig. 2 for sample No. 1 and Fig. 3 for sample No. 2. The variation in the output radiation power of our simple homemade CO_2 laser produced the fairly large fluctuations in photocurrent. Data from only the positive bias (defined as the top of the device mesa biased positively with respect to the bottom contact, upper part of Fig. 1) are shown; the observed photocurrent with negative bias was much smaller (by about a factor of 20) than that of the positive bias.

A single resonant-tunneling feature was observed in the positive $I\text{-}V$ characteristics (at about 0.34 V for sample No. 1 and 0.22V for sample No. 2 — see Figs. 2 and 3). The difference in doping of the wells causes the difference between the RT voltage positions. The less distinct RT feature in sample No. 2 is also attributed to

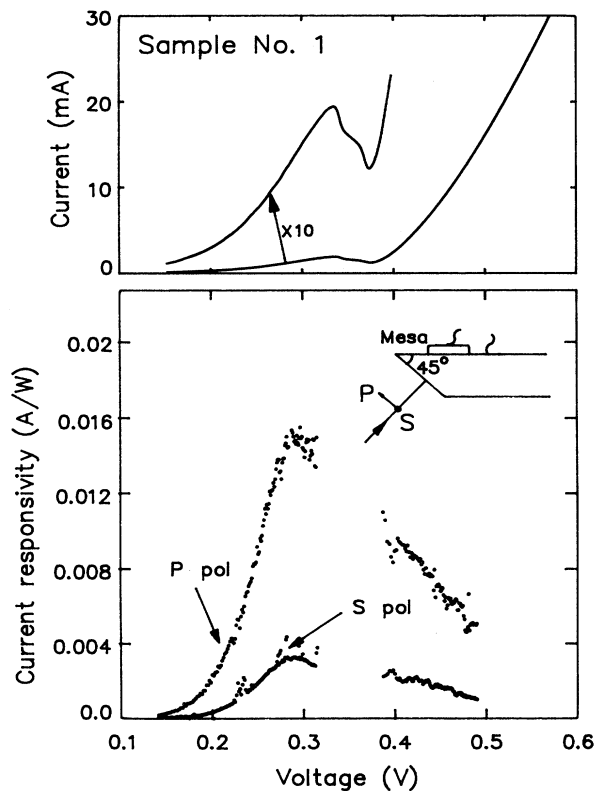


FIG. 2. Current-voltage and photocurrent-voltage characteristics of sample No. 1 at 10 K. Sample No. 1 has a undoped quantum well. The inset shows schematically the measurement geometry.

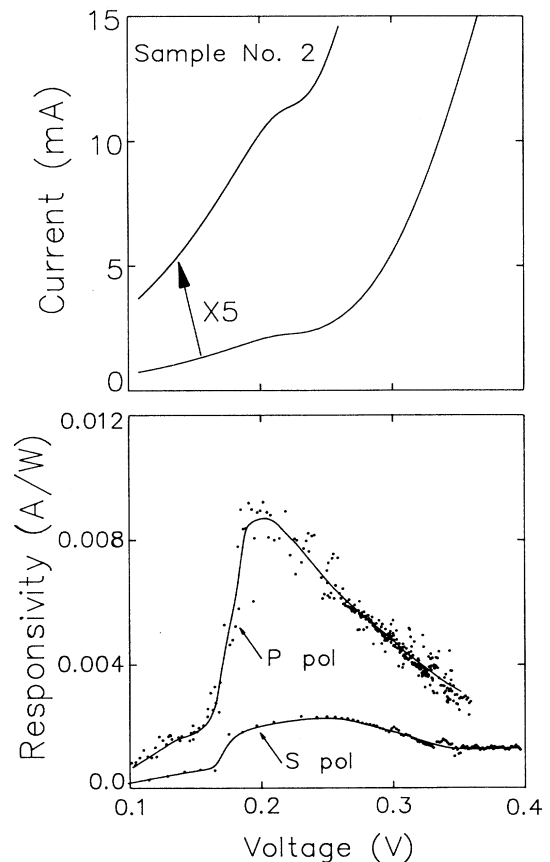


FIG. 3. Current-voltage and photocurrent-voltage characteristics of sample No. 2 at 10 K. Lines in the photocurrent data are drawn to guide the eye. Sample No. 2 has a center δ -doped quantum well with a doping density of about $9 \times 10^{11} \text{ cm}^{-2}$.

the δ doping which partially destroys the perfect one-dimensional nature of the tunneling process.¹⁰ For the P polarization, the peak in the photocurrent occurs at a slightly lower bias than that in I - V (at about 0.3 V for sample No. 1 and at about 0.2 V for sample No. 2); the photocurrent then decreases after the negative differential resistance (NDR) region. For sample No. 1, the NDR region was not accessible experimentally because the measuring circuit became unstable.¹¹ Note that the photocurrent does not vanish after the resonant peak, indicating that there is a substantial electron accumulation (at most a factor of 2 lower than the on-resonance electron accumulation). This implies that the excess current (i.e., the valley current) after the RT current peak is largely due to scattering-assisted RT, for example, scattering by phonons, impurities, interface roughness, and so on. A non-negligible electron accumulation after the RT peak would reduce the observability of the intrinsic bistability.⁵ For the S polarization, which ideally is not expected to induce intersubband transitions because the electric field associated with the CO₂ radiation has a zero component in the epitaxial growth direction,¹² the observed photocurrents were much smaller than those for the P polarization. However, the S photocurrents were not zero, probably because of intersubband transitions induced by imperfection scattering (e.g., interface roughness¹³). Because of the difference in the photocurrent behavior under two polarizations, we attribute the P photocurrent to the intersubband transition from the first resonant state to the second followed by the escape of electrons from the second resonant state. In fact, only a half of the P polarized photon power induces the intersubband photocurrent because of the 45° incidence. Therefore the ratio between P and S photocurrents is actually larger by a factor of 2 than that shown in Figs. 2 and 3. The photocurrent data of the two samples studied here shows that a substantial electron density can be achieved even *without* doping the well. The two samples may, however, not be directly comparable, and the difference in the magnitude of photocurrents may be due to a slight difference in the intersubband transition energies between the two samples, so that 9- μ m photon energy corresponds to a slightly different position with respect to the absorption peak. The linewidth of the absorption is expected to be about 0.014 eV (about one-tenth of the transition energy). Choi *et al.*¹⁴ have shown electron accumulation in undoped QW's previously in a MQW structure. However, their structure addresses the two-dimensional to two-dimensional tunneling, and does not have any structural asymmetry. Therefore, the important points of very different charge accumulation behavior in positive and negative bias as well as charge accumulation in the RT valley could not be addressed in their study.

To make certain that the observed photocurrent is due to the charge build-up in the well, we consider and rule out other possibilities. If the intersubband absorption strongly depends on the electric field, one would expect a strong dependence of the photocurrent on the applied bias. We therefore performed transmission spectrum measurements on the MQW sample and found only

small changes in the intersubband absorption as a function of field. This implies that the field dependence cannot account for our experiments. Another possibility is that electrons in the accumulation region in the emitter immediately before the double-barrier could give rise to a photocurrent, but this photocurrent would exist for both positive and negative bias voltages. Experimentally, we observed a much smaller photocurrent under negative bias. In addition, the photon energy required to induce a photocurrent from the quasi-two-dimensional accumulation electrons would be much larger than the 9- μ m photon energy, and photocurrent from exciting the three-dimensional emitter electrons would be polarization insensitive. We conclude that the observed P-polarized photocurrent is indeed mainly due to the charge build-up and intersubband absorption.

We now consider the RT current density J and the electron accumulation (i.e., two-dimensional number density) in the RT regime quantitatively. We use the expressions for charge build-up in the well similar to those given originally by Goldman, Tsui, and Cunningham.⁵ In the low-temperature limit, the double-barrier RT current and the electron accumulation in the well are easily expressed in terms of the individual transmission coefficients (T_1 and T_2 evaluated at the resonance energy) through the first (emitter) and the second (collector) barriers:¹⁵

$$J = \frac{em}{\pi\hbar^2} \frac{v_R}{2a_{\text{eff}}} \frac{T_1 T_2}{T_1 + T_2} (E_F^{(1)} - \max[E_R, E_F^{(2)}]) \Theta, \quad (1)$$

$$n = D_{2D} \frac{T_1 (E_F^{(1)} - E_R) + T_2 (E_F^{(2)} - \min[E_R, E_F^{(2)}])}{T_1 + T_2} \Theta, \quad (2)$$

where m is the effective mass in the contact, v_R is the velocity of an electron in the resonant state in the tunneling direction, a_{eff} is the effective well width which equals the sum of the well width and the inverses of the imaginary wave vectors in the two barriers,⁷ E_R is the energy of the resonant state, $E_F^{(1,2)}$ are the Fermi energies in the emitter (1) and collector (2), respectively, and $\Theta = \theta(E_R)\theta(E_F^{(1)} - E_R)$, and $D_{2D} = \pi\hbar^2/m$ is the two-dimensional density of states. We have chosen the emitter band edge as the energy reference. The bias voltage dependence is given implicitly in E_R , $E_F^{(2)}$, T_1 and T_2 . The above expressions are valid only in the RT regime which is defined by the two θ functions. The RT current [Eq. (1)] can be derived either from a scattering approach¹⁶ or a sequential transfer Hamiltonian approach.¹⁵ Equation (1) gives the standard RT I - V characteristics, and the electron accumulation [Eq. (2)] behaves similarly to the RT current, although with the peak occurring at a slightly lower voltage.¹⁵ For $E_R > E_F^{(2)}$ (true for bias voltages larger than about 0.1 V in our case), the RT current J is proportional to $(E_F^{(1)} - E_R)T_1 T_2 / (T_1 + T_2)$ and the electron density n is proportional to $(E_F^{(1)} - E_R)T_1 / (T_1 + T_2)$ in the RT regime. Thus, in the limit $T_1 \gg T_2$, a maximum accumulation electron density occurs, and for $T_2 \gg T_1$, a

negligible electron accumulation is expected. Also, J and n behave very similarly as a function of the bias voltage,⁷ except for the missing T_2 in the expression for n . The effect of the missing T_2 is to shift the peak in n to a slightly lower voltage with respect to the peak in J , because T_2 increases as a function of voltage. This behavior is visible in Figs. 2 and 3.

In conclusion, we have measured the intersubband photocurrent from two double-barrier resonant-tunneling samples with doped and undoped quantum wells. The

photocurrent behaves similarly to the resonant-tunneling feature. A simple qualitative theoretical interpretation is in good agreement with experiments. These double-barrier structures may be optimized for fast response ir detection.¹⁷

The authors thank D. Blair, P. Chow-Chong, and P. Marshall for sample preparation. Also, we benefited greatly from many discussions with Dr. G. C. Aers and Dr. J. F. Young.

¹K. K. Choi, B. F. Levine, C. G. Bethea, J. Walker, and R. J. Malik, *Phys. Rev. Lett.* **59**, 2459 (1987).

²B. F. Levine, C. G. Bethea, G. Hasnain, J. Walker, R. J. Malik, and J. M. Vandenberg, *Phys. Rev. Lett.* **63**, 899 (1989).

³M. Helm, P. England, E. Colas, F. DeRosa, and S. J. Allen, Jr., *Phys. Rev. Lett.* **63**, 74 (1989).

⁴B. F. Levine, C. G. Bethea, G. Hasnain, V. O. Shen, E. Pelve, R. R. Abbott, and S. J. Hsieh, *Appl. Phys. Lett.* **56**, 851 (1990), and references therein.

⁵V. J. Goldman, D. C. Tsui, and J. E. Cunningham, *Phys. Rev. Lett.* **58**, 1256 (1987).

⁶M. Tsuchiya, T. Matsusue, and H. Sakaki, *Phys. Rev. Lett.* **59**, 2356 (1987).

⁷J. F. Young, B. W. Wood, G. C. Aers, R. L. S. Devine, H. C. Liu, D. Landheer, M. Buchanan, A. J. SpringThorpe, and P. Mandeville, *Phys. Rev. Lett.* **60**, 2058 (1988).

⁸W. Cai, T. F. Zheng, P. Hu, M. Lax, K. Shum, and R. R. Alfano, *Phys. Rev. Lett.* **65**, 104 (1990).

⁹M. S. Skolnick, D. G. Hayes, P. E. Simmonds, A. W. Higgs, G. W. Smith, H. J. Hutchinson, C. R. Whitehouse, L. Eaves, M. Henini, O. H. Hughes, M. L. Leadbeater, and D. P. Halliday, *Phys. Rev. B* **41**, 10 754 (1990).

¹⁰E. Wolak, K. L. Lear, P. M. Pitner, E. S. Hellman, B. G. Park, T. Weil, and J. S. Harris, Jr., *Appl. Phys. Lett.* **53**, 201 (1988).

¹¹H. C. Liu, *J. Appl. Phys.* **64**, 4792 (1988).

¹²D. D. Coon and R. P. G. Karunasiri, *Appl. Phys. Lett.* **45**, 649 (1984).

¹³H. C. Liu and D. D. Coon, *Superlatt. Microstruct.* **3**, 357 (1987).

¹⁴K. K. Choi, B. F. Levine, C. G. Bethea, and J. Walker, *Appl. Phys. Lett.* **52**, 1979 (1988).

¹⁵H. C. Liu and G. C. Aers, *J. Appl. Phys.* **65**, 4908 (1989).

¹⁶D. D. Coon and H. C. Liu, *Appl. Phys. Lett.* **49**, 94 (1986).

¹⁷D. D. Coon, R. P. G. Karunasiri, and H. C. Liu, *J. Appl. Phys.* **60**, 2636 (1986).